Journal of Chromatography B, 877 (2009) 2664–2672

Contents lists available at ScienceDirect

Journal of Chromatography B

journal homepage: www.elsevier.com/locate/chromb

Review

High-throughput shotgun lipidomics by quadrupole time-of-flight mass spectrometry☆

Marcus Ståhlman[a,1], Christer S. Ejsing[b,1], Kirill Tarasov[c], Jeanna Perman[a], Jan Borén[a], Kim Ekroos[c,*]

[a] Sahlgrenska Center for Cardiovascular and Metabolic Research/Wallenberg Laboratory, Göteborg University, Göteborg, Sweden
[b] Max Planck Institute of Molecular Cell Biology and Genetics, Dresden, Germany
[c] Zora Biosciences, Espoo, Finland

ARTICLE INFO

Article history:
Received 12 December 2008
Accepted 15 February 2009
Available online 24 February 2009

Keywords:
Shotgun lipidomics
Automation
High-throughput
Mass spectrometry
Multiple precursor ion scanning
QqTOF
Normal phase HPLC

ABSTRACT

Technological advances in mass spectrometry and meticulous method development have produced several shotgun lipidomic approaches capable of characterizing lipid species by direct analysis of total lipid extracts. Shotgun lipidomics by hybrid quadrupole time-of-flight mass spectrometry allows the absolute quantification of hundreds of molecular glycerophospholipid species, glycerolipid species, sphingolipid species and sterol lipids. Future applications in clinical cohort studies demand detailed lipid molecule information and the application of high-throughput lipidomics platforms. In this review we describe a novel high-throughput shotgun lipidomic platform based on 96-well robot-assisted lipid extraction, automated sample infusion by mircofluidic-based nanoelectrospray ionization, and quantitative multiple precursor ion scanning analysis on a quadrupole time-of-flight mass spectrometer. Using this platform to compile comprehensive lipid arrays associated with metabolic dysfunctions is a powerful strategy for pinpointing the mechanistic details by which alterations in tissue-specific lipid metabolism are directly linked to the etiology of many lipid-mediated disorders.

Contents

Abbreviations: CE, cholesteryl ester; CID, collision-induced dissociation; DAG, diacylglycerol; ELS, evaporative light scattering; FA N:M, fatty acid comprising N carbon atoms and M double bonds in its hydrocarbon backbone; ESI, electrospray ionization; GPLs, glycerophospholipids; HepG2, human hepatocellular liver carcinoma cell line; HL-1, cardiac muscle cell line; MPIS, multiple precursor ion scanning; MS, mass spectrometry; MS/MS, tandem mass spectrometry; nanoESI, nanoelectrospray ionization; NLS, neutral loss scanning; PC, phosphatidylcholine; PE, phosphatidylethanolamine; PG, phosphatidylglycerol; PI, phosphatidylinositol; PIS, precursor ion scanning; PS, phosphatidylserine; QqTOF, quadrupole time-of-flight; QqQ, triple quadrupole; SM, sphingomyelin; TAG, triacylglycerol; X FA_i–FA_j, a lipid molecule of class X with fatty acid FA_i and FA_j at unidentified positions; X FA_i/FA_j, a lipid molecule of class X with fatty acid FA_i at *sn*-1 position and FA_j at *sn*-2 position (or *sn*-3 position for DAG); SM N:M ;OH, sphingomyelin comprising N carbon atoms and M double bonds and OH hydroxyl groups in the ceramide backbone.

☆ This paper is part of the special issue "Lipidomics: Developments and Applications", X. Han (Guest Editor).

* Corresponding author. Tel.: +358 40 744 8997.
E-mail address: kim.ekroos@zora.fi (K. Ekroos).

[1] These authors contributed equally to this work.

1570-0232/$ – see front matter © 2009 Elsevier B.V. All rights reserved.
doi:10.1016/j.jchromb.2009.02.037

1. Introduction

Dysregulation of lipid metabolism is a critical contributor to the etiology of obesity and related metabolic diseases such as diabetes, fatty liver disease and atherosclerosis. A growing body of evidence demonstrates that lipid metabolism and its complex output of molecular lipid species play a key role in the development of metabolic syndrome [1]. However, it is still unknown how metabolic diseases affect the entire molecular lipid landscape of cells and tissues, and exactly what metabolic ripple effects cause detrimental effects. Lipidomic studies in clinical settings offer a powerful strategy to pinpoint the mechanistic details by which alterations in tissue-specific lipid metabolism are directly integrated into systemic metabolic homeostasis, but necessitate the application of high-throughput mass spectrometric methodology capable of quantifying molecular lipid species on a lipidome-wide scale.

Lipidomics can be defined as a systems-level analysis of lipid species, their abundance, biological activities, and subcellular localization and tissue distribution. The lipidome of eukaryotic cells can consist of thousands of molecular lipid species that constitute membranes, store metabolic energy and function as bioactive molecules [2,3]. Studies of dysfunctional lipid metabolism can be done using a variety of cell culture models, mouse models and tissue samples from humans. Such studies have provided valuable insights into the metabolic consequences of obesity [4–6], diabetes [7] and insulin resistance [8]. In particular mouse models have been applied to assess the molecular mechanisms of lipid disorders, albeit the mechanisms of action in humans might be different. Large-scale clinical cohort studies are therefore necessary for accurate mapping of metabolic disturbances in humans. Applying lipidomic approaches in concert with identification of the phenotypic consequences of genes involved in lipid metabolism has enabled the reconstruction of the lipid metabolic network with increased information content [1,9], and rendered insights into the causative factors of lipid related dysfunctions in humans [10].

Electrospray ionization mass spectrometry is a powerful tool for lipid analysis [11,12] and is typically used in two major ways. Lipid extracts can be separated by liquid chromatography (LC) and eluted lipid species monitored by on-line mass spectrometry [13,14]. LC–MS or LC–MS/MS detection can be performed in combination with normal phase HPLC that allows lipid class separation or with reversed-phase HPLC that allows separation of molecular lipid species [13–17]. However, using these techniques it is difficult to achieve absolute quantification of hundreds of molecular lipid species since endogenous lipid species and lipid standards can elute with different retention times that in turn changes the lipid ionization efficiency. Furthermore, lipidomic analysis can be compromised by carry-over effects on the column, especially if the analyzed samples differ in their abundance and lipid composition. These techniques are also of limited efficacy for high-throughput screens since separating complex lipid mixtures by HPLC is time-consuming.

Alternatively, lipid extracts can be infused directly into a mass spectrometer whereby lipid species can be identified and quantified using specific precursor ion scans (PIS) and neutral loss scans (NLS) [18–20]. Such shotgun lipidomic techniques have been applied for the characterization of glycerophospholipids (GPLs) [19,21–24], ceramides [25], glycerolipids [26] and sterol lipids [27]. For example, phosphatidylcholine (PC) and sphingomyelin (SM) species are readily detected in positive ion mode by PIS m/z 184.07 for the characteristic phosphorylcholine fragment ion released upon collision-induced dissociation (CID) [19,21,24]. In addition, molecular GPLs can be characterized in negative ion mode based on their release of fatty acid fragment ions [28,29].

Shotgun lipidomics was originally executed on triple quadrupole (QqQ) mass spectrometers that offer sensitive and reproducible analysis with a wide dynamic quantification range [20,24]. The instrumental principles and details on quantification of lipid species using QqQ instruments has been discussed elsewhere [21,30]. QqQ instruments allow the acquisition of only a single PIS or NLS per scan, and the analysis must be repeated to profile multiple lipid classes. Shotgun lipidomic analysis by multiple precursor ion scanning (MPIS) was recently developed for hybrid quadrupole time-of-flight (QqTOF) mass spectrometers [19,28]. MPIS enabled the simultaneous acquisition of 40–50 PIS required for the comprehensive characterization of eukaryotic lipidomes in a single analysis [23,28]. Furthermore, the MPIS methodology was recently complemented by dedicated software that enables automated identification of detected lipid species and absolute quantification when applicable internal lipid standards are used [23]. This methodology has been applied in relatively low throughput studies of liver steatosis [8], hyperlipidemia [4] and T cell receptor activation [31].

In this review we describe a novel high-throughput shotgun lipidomic platform based on 96-well robot-assisted lipid extraction, automated sample infusion by mircofluidic-based nanoelectrospray ionization, and quantitative MPIS analysis on a QqTOF mass spectrometer (Fig. 1). We discuss the validation and key features of the methodology, and emphasize practical issues associated with operating the platform. By implementing lipid class separation and fractionation prior to MS analysis, quantitative lipidomic analysis of a wide range of mammalian tissues can be achieved. We highlight the efficacy of this platform by discussing its application for both low-throughput and high-throughput shotgun lipidomics studies.

2. Automated shotgun lipidomics

2.1. 96-Well robot-assisted lipid extraction

Sample preparation is of crucial importance for generating high quality lipidomic datasets. The use of solvents, reagents, sample amounts, internal lipid standards and lipid extraction protocols should be carefully considered in order to optimize the sensitivity, comprehensiveness and the quantification accuracy of the mass spectrometric analysis.

Quantification of lipids can be achieved by profiling analysis, relative quantification and absolute quantification. Absolute quantification (*i.e.* pmol lipid) is the ideal lipidomic data format as it provides information about the stoichiometric relationship between lipid species of different classes. Absolute quantification requires that samples are spiked with defined amounts of an applicable internal lipid standards prior to lipid extraction (usually in the pmol concentration range; and at least one lipid standard per monitored lipid class) [19,23,32]. In addition, the lipid standards should be absent from the sample matrix. This approach will correct for any bias in lipid extraction recovery, lipid class-dependent ionization efficiencies, and improve the accuracy of the quantitative analysis. In comparison, profiling analysis is a qualitative approach performed without lipid standards where only the intensity (or peak area) of detected lipids are compared in order to pinpoint differences that can be targeted for detailed analysis. Relative quantification (*i.e.* fold difference compared to control) is typically performed when only a limited set of internal lipid standards is available [19]. Importantly, both profiling analysis and relative quantification does not provide direct information on the stoichiometric relationship between lipid species, and are prone to poor analytical reproducibility.

Lipids are commonly extracted using traditional Bligh and Dyer [33] or Folch protocols [34] based on liquid–liquid extraction using

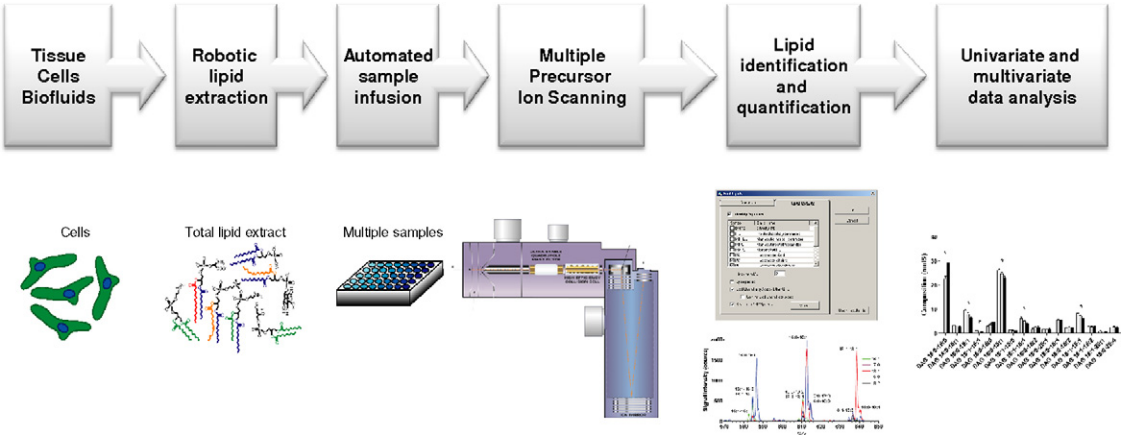

Fig. 1. Schematic outline of the high-throughput shotgun lipidomic platform.

chloroform, methanol and aqueous buffer. These procedures generally allow recovery of most eukaryotic lipids; albeit very polar lipids such as phosphoinositides and complex glycosphingolipids require dedicated extraction methods [35–37]. We emphasize that accurate quantification of lipid species requires the spiking with internal lipid standards prior to extraction in order to correct for biased losses of monitored lipid classes, especially when concentrated samples are investigated. Furthermore, using large volumes of organic solvents (*e.g.* chloroform/methanol (2:1, v/v)) relative to sample lipid content and repeating the lipid extraction of the aqueous phase, result in high lipid recoveries (85–100%). Total lipid extracts are evaporated, and dissolved in chloroform/methanol (1:2, v/v) prior to shotgun lipidomic analysis or HPLC fractionation (see below).

Manual lipid extraction is relatively labor-intensive and prone to errors when hundreds of samples need to be processed for clinical studies. To this end, we have developed an automated lipid extraction procedure in a 96-well plate format. We typically perform lipid extraction using 1.3 ml glass vials inserted in a custom-made aluminum 96-vial rack. Manual interferences in the lipid extraction procedure have been minimized such that all pipetting and sample mixing is performed by the robot. To ensure optimal lipid extraction efficiencies the sample mixing is performed by repeated aspiration and dispensing at varying vertical positions of the glass vials. Isolation of the organic and lipid-enriched phase is done after leaving the samples to phase separate for 5 min without agitation. We note that the lipid extraction can also be performed using high quality organic solvent-resistant plastics including tips, 96-well plates and solution trays. The advantage of this approach is that the procedure becomes less labor-intensive and more cost-effective.

To validate the automated lipid extraction procedure we monitored the extraction recovery and quantification accuracy of lipid species in various sample matrices (*e.g.* cells, tissue homogenates and biofluids). We observed no significant differences in the extraction recovery and quantification accuracy when performing robotic or manual lipid extraction (not shown). Importantly, the robotic lipid extraction had a better analytical reproducibility compared to manual lipid extraction (not shown). Furthermore, the robotic lipid extraction allowed the processing of 96 samples within 6 h.

2.2. Automated sample infusion by mircofluidic-based nanoelectrospray ionization

Shotgun lipidomics has been successfully performed using nanoelectrospray ionization (nanoESI) [19,21]. Conventional nanoESI is sensitive and cost-effective, but requires manual loading of samples into small glass capillary emitters, manual positioning of emitters in front of the mass spectrometer orifice and adjustment of voltage and back pressure to achieve stable ion spray. Automation of nanoESI has been attempted by continuous flow injection for analysis of multiple samples [38]. Drawback of this technique is that all samples are infused through the same capillary emitter, which increases the risk for cross-contamination. An alternative is the automated chip-based nanoESI device: NanoMate TriVersa [39]. Here, the samples are aspirated robotically from a 96- or 384-well plate and infused into the mass spectrometer through separate nozzles on an ESI Chip. Each ESI Chip contains 400 nozzles. ESI Chips are available with nozzles having an inner diameter of 2.5, 4.1 or 5.0 μm. The device eliminates cross-contamination between different samples and allows flow rates between 100 and 250 nL/min depending on ion spray parameters; *e.g.* nozzle diameter, ion spray voltage, back pressure and solvent composition.

For routine lipidomics experiments we dissolve lipid extracts in 5 mM ammonium acetate in chloroform/methanol (1:2, v/v). Samples are infused by the TriVersa NanoMate with a 4.1 μm ESI Chip using ±1.2 kV and 0.2 psi as ion spray voltage and back pressure, respectively. Infusing 10 μl of sample (with a maximum concentration of ~20 μM total lipid or ~0.05 μg extracted protein per μL) allows approximately 67 min of stable ion spray equivalent to a flow rate of 149 nL/min (Fig. 2). The spectral reproducibility achieved using the NanoMate TriVersa gives a relative standard error of approximately 3% in both positive and negative ion mode (not shown). Importantly, this device produces similar lipid profiles as compared to syringe pump-driven capillary interfaces [40] and conventional nanoESI (not shown). We note that several studies have successfully applied the TriVersa NanoMate device for shotgun lipidomics analysis of lipid extracts [4,8,23,31,37,40–42].

A major concern for the handling of lipid extracts in low volumes of volatile chloroform and methanol is sample evaporation. Sealing of 96-well plates with aluminum foil is a prerequisite for minimizing sample evaporation. In addition, the NanoMate TriVersa system has an integrated cooling device to store the sample plate at 4–10 °C during the mass spectrometric analysis. Furthermore, sealed 96-well plates can be stored at −20 °C for up to 4 weeks without noticeable sample evaporation and alterations of the measured lipid composition. The materials of the sample tips (electrical conducting plastic tips) and the ESI Chip does not affect the mass spectrometric analyses.

During method development we optimized the analytical efficacy of the TriVersa NanoMate device by testing the impact of various solvent compositions for sample infusion. For routine application we found that using 5 mM ammonium acetate in chloroform/methanol (1:2, v/v) was the optimal solvent system for our

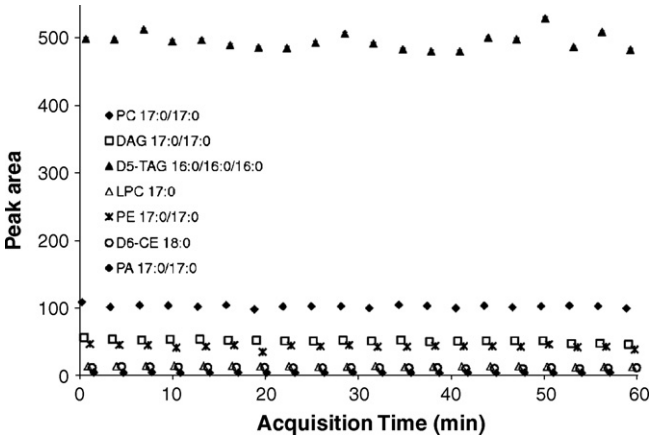

Fig. 2. Monitoring the absolute intensity of lipid precursor as a function of infusion time. 10 μl of total liver lipid extract was infused in positive ion mode at a flow rate of 149 nL/min using a TriVersa NanoMate. MS/MS spectra for each lipid precursor was acquired for 15 s every third minute. The peak area per scan of fragment ions *m/z* of 184.07 (PC 17:0/17:0), *m/z* of 327.29 (DAG 17:0/17:0), *m/z* of 556.54 (D5 TAG 16:0/16:0/16:0), *m/z* of 184.07 (LPC 17:0), *m/z* of 579.43 (PE 17:0/17:0), *m/z* of 375.40 (D6 CE 18:0) and *m/z* of 376.40 (PA 17:0/17:0) are shown. Collision energy was set to 40 eV.

lipidomic analyses. We also tested the efficacy of including isopropanol in the solvent system. When infusing samples in 5 mM ammonium acetate in chloroform/methanol/isopropanol (1:2:4, v/v/v) we observed an improved ion spray stability compared to chloroform/methanol (1:2, v/v). However, for our lipidome-wide analysis we found a minor decrease in overall analytical sensitivity, and a selective ionization of anionic lipids in negative ion mode and neutral sphingolipids in positive ion mode when using chloroform/methanol/isopropanol (1:2:4, v/v/v). Infusion with 5 mM ammonium acetate in chloroform/methanol/isopropanol (1:2:4, v/v/v) also required a higher back pressure for optimal ion spray (*e.g.* ±0.95 kV and 1.25 psi). We note that the analytical sensitivity for anionic lipids in negative ion mode can be further improved using 0.2 mM methylamine in the solvent system [37]. These properties of the TriVersa NanoMate device can be exploited to extend the lipidome coverage of the shotgun analysis, or for detailed structural analysis of a particular lipid species where selective ionization can be used to optimize the analytical sensitivity and specificity [37,40]. Finally, we emphasize that optimal lipidomics analysis is dependent on several parameters of the TriVersa NanoMate device including the type of ESI Chip (*i.e.* nozzle diameter), the ESI Chip to orifice distance and position, pre-piercing of the aluminum foil prior to sample aspiration, the ion spray voltage and back pressure.

2.3. Shotgun lipidomics by MPIS

Development of QqTOF mass spectrometers creates new possibilities for high-throughput shotgun lipidomics [43]. In comparison to QqQ mass spectrometers, QqTOF instruments are equipped with a TOF analyzer instead of the third quadrupole (Q3). The sensitivity of detecting a selected fragment ion (the very essence of PIS) is limited by the duty cycle that can be as low as 5% on QqTOF machines. However, this limitation was overcome when ion trapping and bunching technology was introduced on QSTAR mass spectrometers [44]. Fragment ions of a given *m/z* can be trapped in the collision cell and released as a clustered ion packet into the TOF analyzer. In this way, close to 100% duty cycle can be achieved for low mass fragment ions [45]. This technology has significantly increased the detection sensitivity, allowing QqTOF instruments to reach detection limits at least one order of magnitude better than QqQ instruments (see discussion below).

Other advantages of the QqTOF instruments are the inherent features of the TOF analyzer, such as high mass resolution and accuracy. This allows recording of fragment ions within a narrow mass range (0.1 amu) which provides a high signal-to-noise ratios that minimizes false positive identifications and bias of quantification accuracy [19]. The TOF analyzer allows the recording of numerous PIS in parallel (*i.e.* MPIS). In general, fragment ions with similar masses (*e.g. m/z* 200–350) can be recorded with similar efficiency (*i.e.* similar sensitivity). However, if a wide mass range of fragment ions are to be recorded we recommend performing separate analyses with optimal ion trapping settings for each mass range. We note that in contrast to product ion scanning experiments (*i.e.* multiple reaction monitoring and data-dependent acquisition) where lipid precursors are preselected for fragmentation, the MPIS analysis does not discriminate against detection of potential lipid precursors due to the scanning quadrupole Q1.

For comprehensive glycerophospholipidomics we typically acquire 40–50 PIS scans that covers both fatty acid and lipid headgroup fragment ions within the TOF mass range of *m/z* 150–350 while the quadrupole Q1 is scanning the mass range of *m/z* 450–900 for detection of lipid precursors [19,23]. Molecular GPL species are easily identified by their release of structure-specific fatty acid and head-group fragment ions (Fig. 3) [19,21,28,29,46–54]. Optimal signal response of the MPIS analysis is achieved by adequately optimizing collision energy and collision gas pressure [23]. For the analysis of GPLs, glycerolipids, ceramides and cholesteryl esters (CEs) collision energies of 40–60 eV [23], 25–30 eV, 35–45 eV [55,56] and 25 eV [27], respectively, are commonly used.

We note that prior to any MPIS analysis, QqTOF instruments should be accurately calibrated for optimal performance. To this end, it is advantageous to calibrate the TOF analyzer by recording MS/MS spectra of the synthetic standard PC 16:0–22:6 in either positive or negative ion mode. In positive ion mode, the TOF analyzer is calibrated using the peak intensities of protonated precursor PC 16:0–22:6 with *m/z* 806.5694 and of the phosphorylcholine fragment ion with *m/z* 184.0733. Applying a medium collision energy of 35 eV yields an equal intensity of both ions [57]. In negative ion mode, the TOF analyzer is calibrated by MS/MS of the PC 16:0–22:6 acetate adduct ion having *m/z* 864.5760. Applying a medium collision energy renders characteristic fragment ions corresponding to the demethylated precursor ion [PC 16:0–22:6 $-CH_3]^-$ *m/z* 790.5392 and the fatty acid moieties $[C22:6]^-$ *m/z* 327.2330 and $[C16:0]^-$ *m/z* 255.2330 that allows a three-point calibration of the TOF analyzer [57]. Finally, it is important to avoid saturation of the TOF analyzer during calibration since it affects the mass accuracy.

2.4. Quantitative MPIS analysis

Absolute quantification of lipid species in total lipid extract requires analysis of dilute samples spiked with at least one internal lipid standard per monitored lipid class, and applying isotope correction [20]. Systematic studies of instrument responses using structurally distinct lipid species have demonstrated that ionization efficiency is predominantly dependent on the lipid polar head group and only weakly dependent on the structure of fatty acid moieties [20,22,58]. Ejsing and colleagues recently extended the MPIS analysis to simultaneous quantify molecular PC, phosphatidylethanolamine (PE), phosphatidic acid, phosphatidylserine (PS), phosphatidylglycerol and phosphatidylinositol (PI) species by spiking samples with six distinct lipid class-specific standards having C17:0 moieties and applying automated isotope correction [23]. Our validation of the quantitative MPIS approach has included analysis of equimolar mixtures of PC species (1 μM each) with different acyl chain lengths and number of double bonds that demonstrated no differences in the instrument response when iso-

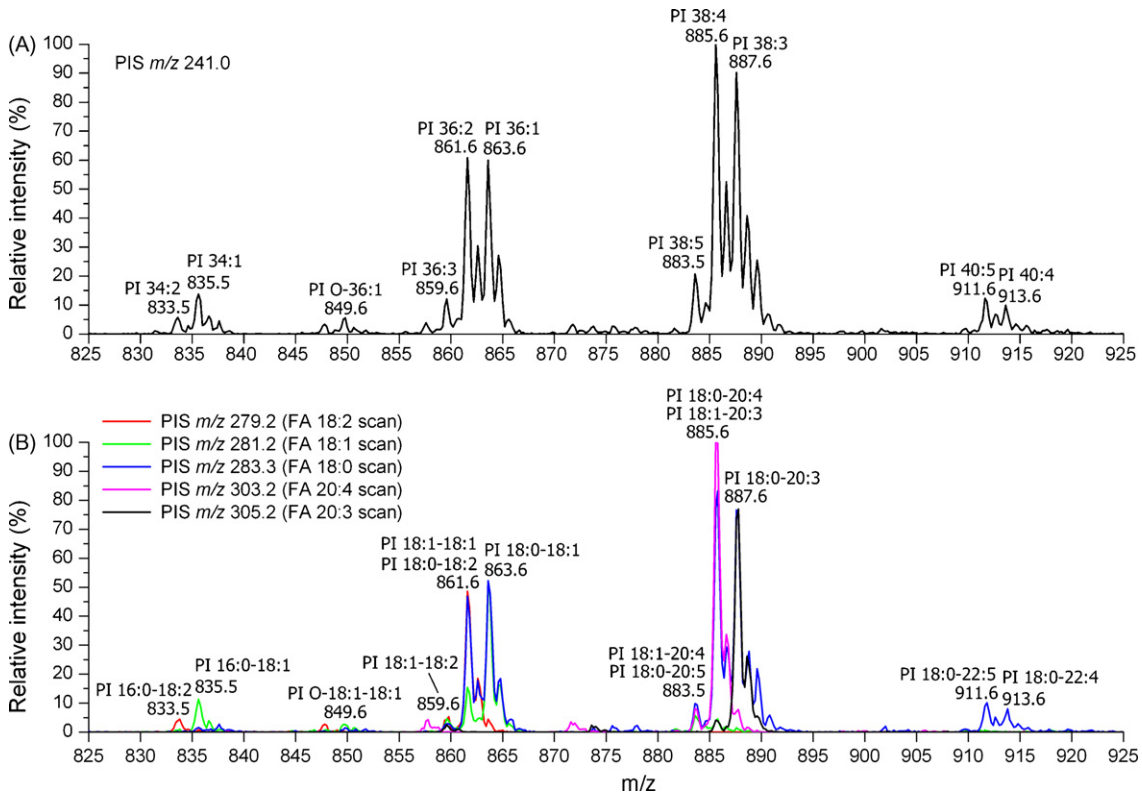

Fig. 3. Spectral profiles obtained by lipid class-specific PIS and lipid species-specific MPIS. (A) PIS *m/z* 241.0 spectrum of bovine liver PI extract acquired in negative ion mode. Detected precursors are annotated as diacyl or ether species using a sum formula. (B) Fatty acid profile of bovine liver PI extract obtained by negative ion mode MPIS analysis. For clarity, only 5 precursor ion spectra (out of 41 acquired) are presented. Identified precursor ions are annotated using a molecular formula that describes the fatty acid moieties of the detected lipid species [23].

tope correction was applied (unpublished data). We note that the quantification accuracy of the lipidomics platform is generally ±5% and in agreement with other shotgun lipidomics approaches [20]. More accurate estimates can probably be achieved by spiking samples with multiple internal lipid standards for each monitored lipid class. However, suitable lipid standards are not always available and customized synthesis is very expensive. We emphasize that evaluation of the performance of any lipidomics platform is always required since quantification accuracy is likely to depend on the ion source (*e.g.* LC, flow injection or direct infusion), sample concentration, MS instrumentation and fragmentation pathways and efficiency.

The dynamic quantification range of MPIS analysis was first assessed by titrating the amount of a total lipid extract relative to a defined amount of spiked internal lipid standard [23]. This analysis demonstrated a linear instrument response for endogenous GPLs over four orders of magnitude corresponding to the concentration range of 10 nM–100 μM total glycerophospholipid. Similar results were obtained in a comparative study of the dynamic quantification range of PIS *m/z* 184.07 analysis on QqQ and QqTOF instruments (Fig. 4). This study showed that both instrumentations featured a 1:1 signal response for two distinct PC molecules over a concentration range of three to four orders of magnitude. This result is in agreement with previous reports [22,23,27,59]. In comparison, the QqTOF MS analysis was 10-fold more sensitive (~2 nM) than QqQ MS analysis due to differences in signal-to-noise ratio in the low pmol range. In contrast, QqQ MS analysis was more accurate at higher sample concentrations (>10 μM) were the QqTOF MS analysis was compromised by detector saturation (at *m/z* 760.6 PC 34:1).

In our laboratory we have obtained similar results for other lipid classes. For example, we evaluated the quantification range for diacylglycerol (DAG) species. To this end, lipid extracts were first diluted and then fractionated by normal phase HPLC (see below). The fractions were spiked with equal concentration of internal standard DAG 17:0/17:0 and analyzed by MPIS analysis in positive ion mode. We simultaneously acquired 40 PIS based on structure-specific fragment ions released from DAG ammonium

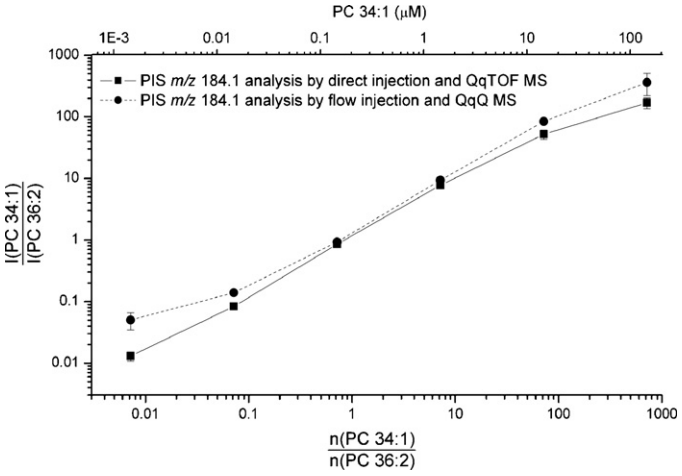

Fig. 4. Dynamic quantification range of PC analysis by QqTOF and QqQ mass spectrometry. Synthetic PC 34:1 was titrated (147 μM to 1.47 nM) relative to a constant amount of synthetic PC 36:2 (205 nM). Lipid mixtures were analyzed in positive ion mode by PIS *m/z* 184.1 using direct infusion by NanoMate and QqTOF mass spectrometry [23], or by flow injection analysis using an Agilent 1100 pump and QqQ mass spectrometry [24]. The upper *x*-axis shows the absolute concentration of PC 34:1. The lower *x*-axis shows the spike amount of PC 34:1 relative to the internal standard PC 36:2. *y*-Axis shows the intensity of PC 34:1 relative to the intensity of PC 36:2. Error bars indicate ±S.D. ($n = 3$ independent analyses).

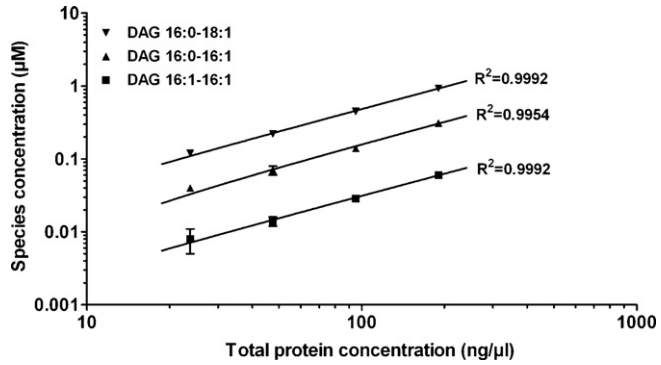

Fig. 5. Dynamic quantification range of DAG analysis. Total lipid extracts of HepG2 cells were diluted and fractionated by normal phase HPLC. Fractions containing DAG were evaporated, reconstituted in 5 mM ammonium acetate in chloroform/methanol (1:2, v/v), spiked with known amount of internal standard DAG 17:0/17:0, and analyzed positive ion mode by MPIS analysis for 40 DAG-derived fragment ions. Collision energy was set to 25 eV. The concentration of endogenous DAG 16:1/16:1, DAG 16:0/16:1 and DAG 16:0/18:1 were estimated by isotope correction of their peak intensity and normalization to the intensity of the internal standard DAG 17:0/17:0 and multiplication with its concentration. The mean values are shown ($n = 4$ independent analyses).

adduct ions. The responses of three endogenous DAG species with up to ~17-fold difference in concentration were assessed (Fig. 5). The experiment demonstrated a linear instrument response for each of the three DAG species within the sample concentration range of 20–200 ng/μl total protein corresponding to 0.01–1 μM DAG. From the similar slope values of the instrument we concluded that DAG 17:0/17:0 is an applicable standard for quantitative MPIS analysis of endogenous DAG species. This experiment also showed that the detection limits for DAG analysis is in the order of 10 nM.

We note that internal lipid standards comprising C17:0 residues (*e.g.* LPA 17:0, DAG 17:0–17:0 and TAG 17:0–17:0–17:0) are applicable for quantitative lipidomics of mouse and human tissues since these lipids are not synthesized in significant amounts. We also note that these GPL standards are detected in the same PIS spectrum (PIS *m/z* 269.25 C17:0) that allows the intensity profile of the standards to be used as a quality control of the analysis. The C17:0 containing lipid standards have successfully been applied in various quantitative lipidomic studies, either by shotgun lipidomics [4,8,42] or LC-based lipidomics [10,60]. An overview of the mode of analysis we use for detection of different lipid species and the respective internal standards are shown in Table 1.

2.5. Automated lipid identification and quantification

Comprehensive and quantitative characterization of lipidomes requires MPIS analysis in positive and negative ion mode. For the comprehensive analysis of a total lipid extract over a hundred PIS spectra are normally recorded. Manual interpretation of such spectral datasets is laborious and time-consuming which makes it impossible to perform large lipidomic studies. Importantly, processing of spectral data requires identification of detected lipid precursors, isotope correction, and quantification by normalization of the intensity of endogenous lipid species to their corresponding internal lipid standards. Development of Lipid Profiler software for automated spectral processing has circumvented these analytical limitations [23]. Lipid Profiler includes all the above-mentioned spectral processing steps and is capable of quantifying molecular lipid species in large lipidomics studies.

Currently, Lipid Profiler affords automated identification of lipid species belonging to 44 distinct lipid classes by cross-correlating spectral information with a lipid library containing fragmentation information on approximately 23,000 lipid species (Eva Duchoslav, personal communication). The software allows identification of the lipid precursor detected using several analytical modes; including survey MS scans (*e.g.* TOF MS), PIS, MPIS [23], data-dependent acquisition [18] and multiple reaction monitoring (MRM) acquired by direct injection, flow injection or LC–MS/MS. In addition, Lipid Profiler also allows the processing of QqQ and ion trap data [61]. The lipid identification considers precursor mass, charge state, and characteristic fragment ions and neutral loss information attributed characteristic lipid class-specific head groups, fatty acid moieties or long chain base (LCB) residues. Processed data are written into a text file. Results from different samples are readily reviewed by automated alignment of identified lipid species and their intensity (or amount) with links to the acquired mass spectra. Finally, the generated data can be exported for further data processing using multivariate data analysis routines [62].

2.6. Shotgun lipidomics in combination with normal phase HPLC

Mammalian tissues, cells and biofluids comprise different molecular lipid compositions. For example, human liver contains predominantly GPLs: approximately 44% PC, 28% PE, 9% PI, 3% PS, 5% SM and 4% cardiolipin, whereas human kidney comprise approximately 34% PC, 27% PE, 6% PI, 7% PS, 12% SM and 7% cardiolipin [63]. Human liver may comprise approximately 8–63% TAG of total lipids [64], whereas adipose tissue comprises about 95% TAG and 5% other lipid classes [65]. Quantitative lipidomic analyses of liver and kidney are readily performed using shotgun lipidomics approaches. However, comprehensive monitoring of minor lipid species in adipose tissue (and TAG rich liver tissue) requires that TAG is removed from the samples prior to any type of lipidomic analysis. To this end, we have employed a normal phase HPLC routine to fractionate individual lipid classes of interest [66,67].

We have validated the lipid class fractionation using HepG2 liver cells, where we compared the molecular composition of lipid species analyzed by shotgun lipidomic analysis of total lipid extracts or after HPLC fractionation. A comparison of the CE and DAG composition from a total lipid extract of HepG2 cells, obtained using the outlined shotgun lipidomics approach, with the profiles generated after normal phase HPLC fractionation of the same lipid

Table 1
Analytical settings used for detection of lipid species.

Lipid class	Analysis	References	Internal standard
PC	+PIS *m/z* 184.07[a]	[21,23]	D(9)-PC 16:0–16:0
	−MPIS		PC 17:0–17:0
PE	−MPIS	[23]	PE 17:0–17:0
PS	−MPIS	[23]	PS 17:0–17:0
PA	−MPIS	[23]	PA 17:0–17:0
PI	−MPIS	[23]	PI 17:0–17:0
PG	−MPIS	[23]	PG 17:0–17:0
LPC	+PIS *m/z* 184.07[a]	[19,21]	LPC 17:0
	−MPIS[b]		
SM	+PIS *m/z* 184.07[a]	[21]	SM 17:0
DAG	+MPIS[c]		DAG 17:0–17:0
TAG	+MPIS[d]		TAG 17:0–17:0–17:0
CE	+PIS *m/z* 369.35	[27]	CE 17:0
Cholesterol	+PIS *m/z* 369.35[e]	[27]	D(7)-FC
CER	+PIS *m/z* 264.27	[56]	CER 17:0
	+PIS *m/z* 266.28		

[a] PIS *m/z* 184.07 analysis; simultaneous detection of PC and SM species; allows only sum composition nomenclature (*e.g.* PC 34:1, SM 34:1;2).

[b] −MPIS analysis; in this analysis LPEs, LPAs, LPGs, LPIs and LPSs are also detected.

[c] +MPIS analysis; structure-specific fragment ions released from DAG–ammonium adduct ions selected for PIS analysis.

[d] +MPIS analysis; structure-specific fragment ions released from TAG–ammonium adduct ions selected for PIS analysis.

[e] +PIS *m/z* 369.35 analysis; cholesterol is converted to cholesteryl ester by acetyl chloride derivatization.

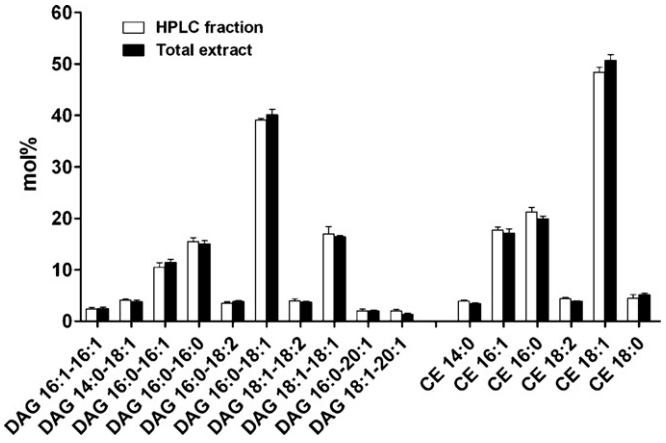

Fig. 6. Comparing the molecular composition of CE and DAG species in total lipid extracts and corresponding HPLC fractions of the total lipid extracts. The molecular lipid composition of CE and DAG were identical thereby no preferential loss of lipid species during the HPLC fractionation. 40 different monoacyl fragment ions recorded by MPIS analysis. PIS m/z 369.3 was used for detection of CE in positive ion mode. Collision energy was set to 25 eV. The values show the mean ± S.D. (n = 5).

extract is illustrated in Fig. 6. This analysis revealed that the molecular composition of molecular DAG and CE species are not affected by the HPLC separation. Furthermore, direct analysis of total lipid extracts by PIS estimated the total amount of CE in HepG2 cells to be 57 nmol/mg protein. In comparison, quantification using evaporative light scattering (ELS) detection together with the HPLC fractionation determined the total amount of CE to be 53 nmol/mg protein. Thus, normal phase HPLC lipid class fractionation can be used in concert with MS-based lipidomic analyses for identification and quantification of minor lipids in complex sample matrices such as adipose tissue (not shown). Another advantage is that the HPLC system helps validate the lipid quantification through the use of two independent detector systems.

3. From low-throughput to high-throughput shotgun lipidomics studies

Cardiac ischemia is associated with an accumulation of lipids in the heart [68]. It has been demonstrated that cardiac myocytes secrete apolipoprotein B-containing lipoproteins following hypoxia. It is still unclear why, but it is believed that their function may be involved in removing accumulating TAG when cellular β-oxidation of fatty acids is impaired during hypoxia. HL-1 cardiomyocytes represent an applicable model for investigating the impact of hypoxia on lipid accumulation since this cell line can express cardiotypic phenotypes that are comparable to primary cardiomyocytes [69]. We performed a shotgun lipidomic study of hypoxia exposed HL-1 cells to pinpoint the hypoxia-induced perturbations of molecular lipid composition. Following hypoxia treatment HL-1 cells were subjected to robotic lipid extraction. Next, aliquots of total lipid extracts were subjected to normal phase HPLC for quantification and fractionation of apolar lipid classes. Another aliquot of total lipid extracts was directly analyzed by quantitative MPIS analysis in negative ion mode for characterization of GPL species [19,23]. In total 150 molecular lipids were quantified.

Quantification of apolar lipid classes using the HPLC procedure showed significant elevations of TAG levels in cells exposed to hypoxia (not shown). A similar TAG accumulation was previously demonstrated for macrophages [70]. No significant alterations in the absolute levels of DAG and CE species were observed. Interestingly, the analysis of DAG showed a significant alteration in their molecular composition after hypoxia for 4 and 8 h (Fig. 7A). Hypoxia resulted in a significant increase in saturated DAG 16:0–16:0 offset by a reduction in monounsaturated DAG 16:0–18:1 and DAG 16:0–16:1. Emulating the fatty acid profile of all detected DAG species demonstrated that the level of fatty acid saturation was primarily attributed to the accumulation of C16:0 and a reduction of C16:1 and C18:1 (Fig. 7B). Interestingly, no significant changes were observed in the molecular composition of CE species (not shown). In contrast, both PC and PE species showed a decrease in the abundance of C16:1 containing species and a concomitant increase in the levels of C18:2 (not shown); attributed predominately to PC 16:0–18:2 and PC 18:0–18:2 (not shown).

This low throughput lipidomics study demonstrates the efficacy of the lipidomics platform for accurately pinpointing subtle alterations in molecular lipid composition after hypoxic exposure. The lipidome perturbation may have important physiological consequences since the saturation index of GPL is known to affect membrane dynamics, and similar alterations have been observed in different disease states [71]. Since desaturation of fatty acids is catalyzed by stearoyl-CoA desaturases that utilize NAD(P)H as electron donor [71] it is possible that the hypoxia-induced increase in saturated fatty acids is partly attributed to reduced availability of molecular oxygen for this biochemical process.

These results provide novel insight into the underlying biological mechanisms of hypoxia, and also shed light on the discovery of novel disease-related lipid biomarkers and potential drug targets. However, if biomarkers and drug targets are to be discovered and verified in humans, large clinical cohorts are required. At this point, high-throughput and automation become necessities. It is important for such studies that the data quality is uncom-

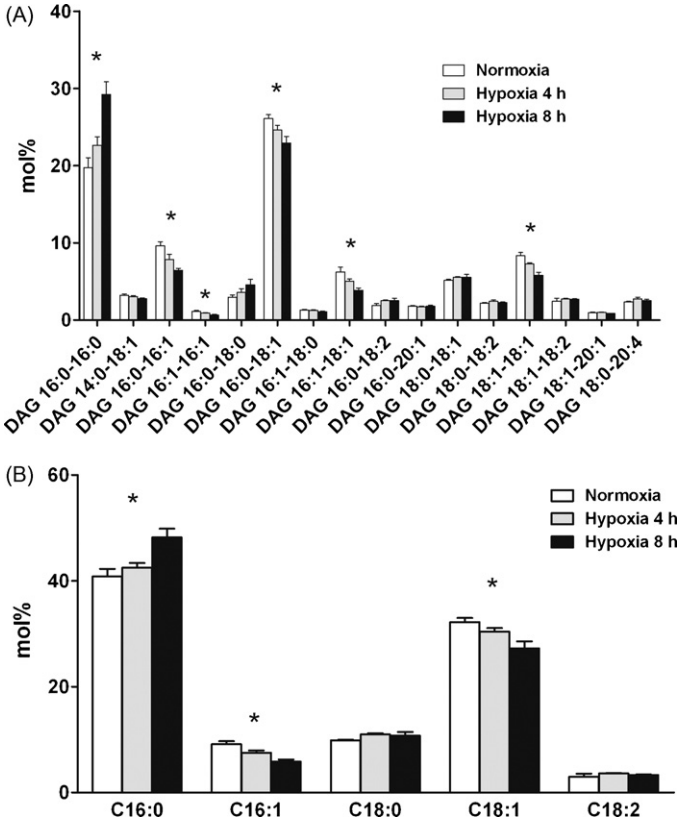

Fig. 7. Hypoxia-induced perturbations of molecular DAG composition. After HPLC fractionation of HL-1 total lipid extract, DAGs were analyzed by MPIS analysis. (A) Exposure to hypoxia resulted in several significant alterations in the molecular composition of DAG species. (B) Effect of hypoxia on fatty acid composition of the DAG species. Hypoxia resulted in decreases in unsaturated fatty acids and increases in saturated species. 40 different monoacyl fragment ions were recorded by MPIS analysis in positive ion mode. Collision energy was set to 25 eV. Values shows the mean ± S.D. (n = 3), $^*p < 0.01$ (Student's t-test).

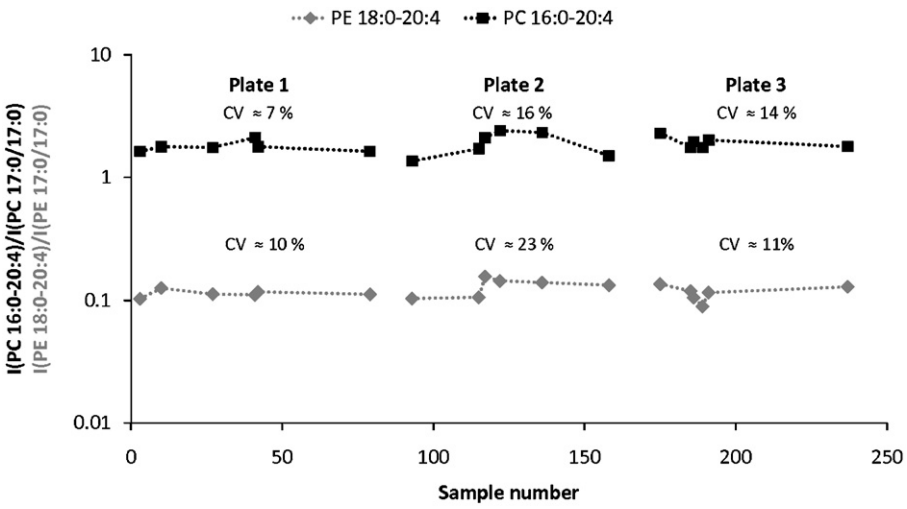

Fig. 8. Evaluating the analytical variation in a large-scale lipidomics study. 237 samples distributed in 3 distinct 96-well plates were processed by robotic lipid extraction and analyzed by negative ion mode MPIS over a 5-day period. Control plasma samples (6 samples per 96-well plate) were randomly measured during the sequence. The relative intensity of PC 16:0–20:4 and PE 18:0–20:4 (normalized to the respective internal standard) in control plasma samples were monitored as a function of sample number in order to estimate variation of the shotgun lipidomics platform.

promised as compared to low-throughput and focused lipidomics studies.

In large-scale clinical studies we typically monitor hundreds of molecular lipid species in several hundred samples using the outlined high-throughput shotgun lipidomics platform. For routine application we include several control samples to track the quality of the analysis. Fig. 8 shows an example of the analytical variation between 237 samples analyzed over a 5-day period (samples were loaded in three distinct 96-well plates). This result demonstrates that the lipidomics platform features a high analytical reproducibility with a relative standard error in the order of 15% throughout a 5-day period. In summary, the analytical approach facilitates high-throughput shotgun lipidomics without compromising the analytical quality and lends itself to high quality lipidomic analyses in large-scale clinical studies.

4. Conclusions and future directions

Here we have described a novel high-throughput shotgun lipidomics platform based on 96-well robot-assisted lipid extraction, automated sample infusion by mircofluidics-based nanoelectrospray ionization, and quantitative MPIS analysis by QqTOF mass spectrometry. This platform has enabled the quantification of several hundreds of molecular lipid species from minute amounts of sample. The efficacy of this approach has been demonstrated by its ability to analyze diverse and complex sample matrices including adipose and liver tissue. Applying lipidomics to clinical cohort studies established a new strategy for pinpointing the mechanistic details by which alterations in tissue-specific lipid metabolism are linked to systemic metabolic homeostasis and disease states.

The methodology offers the possibility to characterize molecular lipid species (*e.g.* PC 18:1–18:1 and PC 18:0–18:2) instead of identifying lipids by only sum composition (*e.g.* PC 36:2). Similar to other lipidomics techniques, the MPIS methodology is unable to accurately quantify positional isomeric lipid molecules where the position of the fatty acid moieties are interchanged (*e.g.* PC 16:1/18:1 and PC 18:1/16:1) [28]. Furthermore, a technical caveat of most shotgun lipidomics platforms is the inability to directly determine the position and configuration (*cis* or *trans*) of double bonds within the fatty acid moieties of lipid species. To this end, ozone-induced dissociation (OzID) of double bonds might offer a promising solution [72–74]. Thomas and colleagues have demonstrated that the regio-isomeric ions PC 18:1(9*Z*)/18:1(9*Z*) and PC 18:1(6*Z*)/18:1(6*Z*) can be distinguished by OzID. Interestingly, close to complete structural information on lipid species can now be determined by shotgun mass spectrometry. Notably, similar information could be obtained, but only through very labor-intensive sample pre-fractionation and gas chromatography–mass spectrometry. This conventional approach, however, fails to decipher to which lipid species the fatty acid moieties are attached to since structural information is lost during sample hydrolysis. Interestingly, OzID can also be applied in conjunction with shotgun lipidomics or LC–MS/MS analysis. A future challenge will be to implement OzID into the high-throughput shotgun lipidomics platform. Since OzID renders additional fragmentation events, this approach will demand additional developments of mass spectrometric instrumentations and software. In addition, techniques such as OzID will help understand the gas phase chemistry of lipids and possibly extend the structural characterization of molecular lipid species.

In summary, the shotgun lipidomic platform described herein is applicable for molecular characterization and quantification of lipid species on a lipidome-wide scale. The integration of robotic lipid extraction, automated sample infusion together with quantitative MPIS analysis and software-assisted data analysis have enabled higher sample throughputs as required for large sample number clinical studies. We expect that 50 samples can be analyzed per day; from automated sample preparation including lipid extraction to reporting the results. We believe that the methodology will help advance our understanding of the physiological functions of lipid species, and delineate the pathophysiology of multiple lipid-related diseases such as obesity, atherosclerosis, diabetes and cancer. Integrated with other *omics* strategies this platform will offer a new avenue for dissecting and improving disease diagnosis and prevention.

Acknowledgements

We are grateful to Dr. G. Liebisch (University of Regensburg, Germany) for the contribution of QqQ data, and Dr. B. Simons (MDS Analytical Technologies) for data showing the ion spray sta-

bility. We thank Drs. Andrej Shevchenko and Kai Simons (Max Planck Institute of Molecular Cell Biology and Genetics) for their constructive comments. We thank Drs. Eva Duchoslav, Igor Chernushevich, Ron Bonner (MDS Analytical Technologies) and Gary Impey (Applied Biosystems) for expert advice on Lipid Profiler and QqTOF mass spectrometry. We are grateful to Mark Baumert and Reinaldo Almeida (Advion Biosciences, Inc.) for their expert advice on NanoMate TriVersa system operation. We also thank all members of our laboratories for valuable discussions and suggestions.

References

[1] H. Cao, K. Gerhold, J.R. Mayers, M.M. Wiest, S.M. Watkins, G.S. Hotamisligil, Cell 134 (2008) 933.
[2] G. van Meer, D.R. Voelker, G.W. Feigenson, Nat. Rev. Mol. Cell. Biol. 9 (2008) 112.
[3] M.P. Wymann, R. Schneiter, Nat. Rev. Mol. Cell. Biol. 9 (2008) 162.
[4] C.J. Lelliott, A. Ljungberg, A. Ahnmark, L. William-Olsson, K. Ekroos, A. Elmgren, G. Arnerup, C.C. Shoulders, J. Oscarsson, D. Linden, Arterioscler. Thromb. Vasc. Biol. 27 (2007) 2707.
[5] A.D. Watson, J. Lipid. Res. 47 (2006) 2101.
[6] M. Kolak, J. Westerbacka, V.R. Velagapudi, D. Wagsater, L. Yetukuri, J. Makkonen, A. Rissanen, A.M. Hakkinen, M. Lindell, R. Bergholm, A. Hamsten, P. Eriksson, R.M. Fisher, M. Oresic, H. Yki-Jarvinen, Diabetes 56 (2007) 1960.
[7] R.W. Gross, X. Han, Methods Enzymol. 433 (2007) 73.
[8] D. Linden, L. William-Olsson, A. Ahnmark, K. Ekroos, C. Hallberg, H.P. Sjogren, B. Becker, L. Svensson, J.C. Clapham, J. Oscarsson, S. Schreyer, FASEB J. 20 (2006) 434.
[9] L. Yetukuri, M. Katajamaa, G. Medina-Gomez, T. Seppanen-Laakso, A. Vidal-Puig, M. Oresic, BMC Syst. Biol. 1 (2007) 12.
[10] R. Laaksonen, M. Katajamaa, H. Paiva, M. Sysi-Aho, L. Saarinen, P. Junni, D. Lutjohann, J. Smet, R. Van Coster, T. Seppanen-Laakso, T. Lehtimaki, J. Soini, M. Oresic, PLoS ONE 1 (2006) e97.
[11] M.R. Wenk, Nat. Rev. Drug Discov. 4 (2005) 594.
[12] X. Han, R.W. Gross, Expert Rev. Proteomics 2 (2005) 253.
[13] A. Kuksis, L. Marai, J.J. Myher, Lipids 26 (1991) 240.
[14] H. Ogiso, T. Suzuki, R. Taguchi, Anal. Biochem. 375 (2008) 124.
[15] R. Taguchi, T. Houjou, H. Nakanishi, T. Yamazaki, M. Ishida, M. Imagawa, T. Shimizu, J. Chromatogr. B: Analyt. Technol. Biomed. Life Sci. 823 (2005) 26.
[16] S. Uran, A. Larsen, P.B. Jacobsen, T. Skotland, J. Chromatogr. B: Biomed. Sci. Appl. 758 (2001) 265.
[17] R. Taguchi, M. Nishijima, T. Shimizu, Methods Enzymol. 432 (2007) 185.
[18] D. Schwudke, J. Oegema, L. Burton, E. Entchev, J.T. Hannich, C.S. Ejsing, T. Kurzchalia, A. Shevchenko, Anal. Chem. 78 (2006) 585.
[19] K. Ekroos, I.V. Chernushevich, K. Simons, A. Shevchenko, Anal. Chem. 74 (2002) 941.
[20] X. Han, R.W. Gross, Mass Spectrom. Rev. 24 (2005) 367.
[21] B. Brugger, G. Erben, R. Sandhoff, F.T. Wieland, W.D. Lehmann, Proc. Natl. Acad. Sci. U.S.A. 94 (1997) 2339.
[22] X. Han, R.W. Gross, Proc. Natl. Acad. Sci. U.S.A. 91 (1994) 10635.
[23] C.S. Ejsing, E. Duchoslav, J. Sampaio, K. Simons, R. Bonner, C. Thiele, K. Ekroos, A. Shevchenko, Anal. Chem. 78 (2006) 6202.
[24] G. Liebisch, B. Lieser, J. Rathenberg, W. Drobnik, G. Schmitz, Biochim. Biophys. Acta 1686 (2004) 108.
[25] X. Han, Anal. Biochem. 302 (2002) 199.
[26] A.M. McAnoy, C.C. Wu, R.C. Murphy, J. Am. Soc. Mass Spectrom. 16 (2005) 1498.
[27] G. Liebisch, M. Binder, R. Schifferer, T. Langmann, B. Schulz, G. Schmitz, Biochim. Biophys. Acta 1761 (2006) 121.
[28] K. Ekroos, C.S. Ejsing, U. Bahr, M. Karas, K. Simons, A. Shevchenko, J. Lipid Res. 44 (2003) 2181.
[29] F.F. Hsu, J. Turk, J. Am. Soc. Mass Spectrom. 11 (2000) 892.
[30] M. Koivusalo, P. Haimi, L. Heikinheimo, R. Kostiainen, P. Somerharju, J. Lipid Res. 42 (2001) 663.
[31] T. Zech, C.S. Ejsing, K. Gaus, B. de Wet, A. Shevchenko, K. Simons, T. Harder, EMBO J. (2009).
[32] X. Han, Front. Biosci. 12 (2007) 2601.
[33] E.G. Bligh, W.J. Dyer, Can. J. Biochem. Physiol. 37 (1959) 911.
[34] J. Folch, M. Lees, G.H. Sloane Stanley, J. Biol. Chem. 226 (1957) 497.
[35] T.R. Pettitt, S.K. Dove, A. Lubben, S.D. Calaminus, M.J. Wakelam, J. Lipid Res. 47 (2006) 1588.
[36] A.H. Merrill Jr., M.C. Sullards, J.C. Allegood, S. Kelly, E. Wang, Methods 36 (2005) 207.
[37] C.S. Ejsing, J.L. Sampaio, V. Surendranath, E. Duchoslav, K. Ekroos, R.W. Klemm, K. Simons, A. Shevchenko, Proc. Natl. Acad. Sci. U.S.A. (2009).
[38] S. Geromanos, J. Philip, G. Freckleton, P. Tempst, Rapid Commun. Mass Spectrom. 12 (1998) 551.
[39] C.K. Van Pelt, S. Zhang, E. Fung, I. Chu, T. Liu, C. Li, W.A. Korfmacher, J. Henion, Rapid Commun. Mass Spectrom. 17 (2003) 1573.
[40] X. Han, K. Yang, R.W. Gross, Rapid Commun. Mass Spectrom. 22 (2008) 2115.
[41] Z. Vukelic, M. Zarei, J. Peter-Katalinic, A.D. Zamfir, J. Chromatogr. A 1130 (2006) 238.
[42] T.W. Mitchell, K. Ekroos, S.J. Blanksby, A.J. Hulbert, P.L. Else, J. Exp. Biol. 210 (2007) 3440.
[43] H.R. Morris, T. Paxton, A. Dell, J. Langhorne, M. Berg, R.S. Bordoli, J. Hoyes, R.H. Bateman, Rapid Commun. Mass Spectrom. 10 (1996) 889.
[44] I.V. Chernushevich, Eur. J. Mass Spectrom. 6 (2000) 471.
[45] I.V. Chernushevich, A.V. Loboda, B.A. Thomson, J. Mass Spectrom. 36 (2001) 849.
[46] F.F. Hsu, J. Turk, J. Am. Soc. Mass Spectrom. 14 (2003) 352.
[47] F.F. Hsu, J. Turk, A.K. Thukkani, M.C. Messner, K.R. Wildsmith, D.A. Ford, J. Mass Spectrom. 38 (2003) 752.
[48] F.F. Hsu, J. Turk, J. Am. Soc. Mass Spectrom. 11 (2000) 986.
[49] F.F. Hsu, J. Turk, J. Am. Soc. Mass Spectrom. 11 (2000) 437.
[50] F.F. Hsu, J. Turk, J. Mass Spectrom. 35 (2000) 595.
[51] F.F. Hsu, J. Turk, J. Am. Soc. Mass Spectrom. 11 (2000) 797.
[52] A. Larsen, S. Uran, P.B. Jacobsen, T. Skotland, Rapid Commun. Mass Spectrom. 15 (2001) 2393.
[53] J.L. Kerwin, A.R. Tuininga, L.H. Ericsson, J. Lipid Res. 35 (1994) 1102.
[54] X. Han, R.W. Gross, J. Am. Soc. Mass Spectrom. 6 (1995) 1202.
[55] M.C. Sullards, Methods Enzymol. 312 (2000) 32.
[56] G. Liebisch, W. Drobnik, M. Reil, B. Trumbach, R. Arnecke, B. Olgemoller, A. Roscher, G. Schmitz, J. Lipid Res. 40 (1999) 1539.
[57] K. Ekroos, A. Shevchenko, Rapid Commun. Mass Spectrom. 16 (2002) 1254.
[58] M. Hermansson, A. Uphoff, R. Kakela, P. Somerharju, Anal. Chem. 77 (2005) 2166.
[59] C.J. DeLong, P.R. Baker, M. Samuel, Z. Cui, M.J. Thomas, J. Lipid Res. 42 (2001) 1959.
[60] G. Medina-Gomez, S.L. Gray, L. Yetukuri, K. Shimomura, S. Virtue, M. Campbell, R.K. Curtis, M. Jimenez-Linan, M. Blount, G.S. Yeo, M. Lopez, T. Seppanen-Laakso, F.M. Ashcroft, M. Oresic, A. Vidal-Puig, PLoS Genet. 3 (2007) e64.
[61] R.C. Murphy, P.F. James, A.M. McAnoy, J. Krank, E. Duchoslav, R.M. Barkley, Anal. Biochem. 366 (2007) 59.
[62] G. Ivosev, L. Burton, R. Bonner, Anal. Chem. 80 (2008) 4933.
[63] G. Rouser, G. Simon, G. Kritchevsky, Lipids 4 (1969) 599.
[64] P.O. Kwiterovich Jr., H.R. Sloan, D.S. Fredrickson, J. Lipid Res. 11 (1970) 322.
[65] D.R. Body, Prog. Lipid Res. 27 (1988) 39.
[66] R. Homan, M.K. Anderson, J. Chromatogr. B: Biomed. Sci. Appl. 708 (1998) 21.
[67] C. Silversand, C. Haux, J. Chromatogr. B: Biomed. Sci. Appl. 703 (1997) 7.
[68] J.M. Huss, F.H. Levy, D.P. Kelly, J. Biol. Chem. 276 (2001) 27605.
[69] W.C. Claycomb, N.A. Lanson Jr., B.S. Stallworth, D.B. Egeland, J.B. Delcarpio, A. Bahinski, N.J. Izzo Jr., Proc. Natl. Acad. Sci. U.S.A. 95 (1998) 2979.
[70] P. Bostrom, B. Magnusson, P.A. Svensson, O. Wiklund, J. Boren, L.M. Carlsson, M. Stahlman, S.O. Olofsson, L.M. Hulten, Arterioscler. Thromb. Vasc. Biol. 26 (2006) 1871.
[71] J.M. Ntambi, Prog. Lipid Res. 34 (1995) 139.
[72] M.C. Thomas, T.W. Mitchell, D.G. Harman, J.M. Deeley, J.R. Nealon, S.J. Blanksby, Anal. Chem. 80 (2008) 303.
[73] M.C. Thomas, T.W. Mitchell, D.G. Harman, J.M. Deeley, R.C. Murphy, S.J. Blanksby, Anal. Chem. 79 (2007) 5013.
[74] M.C. Thomas, T.W. Mitchell, S.J. Blanksby, J. Am. Chem. Soc. 128 (2006) 58.